

Experimental and Theoretical Study to Minimize the Cooling Load by Using a New Alternatives in a Space located in Baghdad City

Dr. Ali Hussain Tarrad
Mech. Eng. Dept.
AL-Mustansiriya Univ.
Baghdad-Iraq

Dr. Fouad Alwan Saleh
Mech. Eng. Dept.
AL-Mustansiriya Univ.
Baghdad-Iraq

Wathiq Abdullah Ali
Mech. Eng. Dept.
AL-Mustansiriya Univ.
Baghdad-Iraq

Abstract

The present investigation is concerned with the alternatives used for the cooling load reduction of a space in Baghdad. A numerical and experimental study has been accomplished in Baghdad during July and August of 2008 with the application of a new technique by a suitable alternative for minimizing the cooling load. In the experimental side of this work, a vertical aluminum flat plate is situated on the eastern and southern walls. This sheet is extended into the under ground to a depth of (1) m of a cube test room having (1) m³ size. The experimental data showed that the indoor temperature reduced from (34.5) °C to (31.7) °C and (29.9) °C when using aluminum plate with air gap and glass wool insulation respectively. The heat flux on the southern wall reduced by (23.5%) and (33.7%) for air gap and glass wool respectively. The corresponding reductions on the eastern wall were (20%) and (29.8%) for air gap and glass wool respectively.

A numerical simulation two-dimensional model was performed applying a finite difference technique implemented in a sophisticated MATLAB program. The results of thermal simulations have revealed that the system can significantly reduce the building cooling load when the suggested alternatives have been applied. Finally, it was found that the numerical model was in a good agreement with the experimental data with a maximum discrepancy of (5 %) for the heat flux at the exposed walls.

الخلاصة

يهتم البحث الحالي بالبدائل المستخدمة لتقليل حمل التبريد لحيز في مدينة بغداد. تم إعداد دراسة عددية وتجريبية في مدينة بغداد خلال شهري تموز وأب من عام (2008) بتطبيق تقنية جديدة باستخدام بديل ملأ لتقليل حمل التبريد. في الجانب العملي من هذا البحث، تم تثبيت صفيحة معدنية مصنوعة من الألمنيوم بسمك (1) ملم على الجدران المواجهة للشرق والجنوب من حيز مكعب الشكل بحجم (1) م³ وتمتد تحت الأرض بعمق (1) م. لقد بينت النتائج إن درجة حرارة الحيز انخفضت من (34.5) م° إلى (31.7) م° و (29.9) م° عند تثبيت الصفيحة ووجود فجوة من الهواء أو طبقة من الصوف الزجاجي محصورة بين الجدار والصفيحة على التعاقب. تم تخفيض الفيض الحراري

المسلط على الجدار المواجه للجنوب بمقدار (23.5%) و(33.7%) لحالة طبقة الهواء والصفوف الزجاجي مع الصفيحة المعدنية على التعاقب. الانخفاض المناظر للجدار المواجه للشرق كان (20%) و(29.8%) لحالة فجوة الهواء والصفوف الزجاجي مع الصفيحة المعدنية على التوالي. في الجانب النظري تم بناء نموذج عددي ثنائي الأبعاد بتطبيق تقنية الفروقات المتناهية أعدت ضمن برنامج تم بناؤه لهذا الغرض. النتائج النظرية للمحاكاة بينت إمكانية تقليل حمل التبريد للحيث عند استخدام البدائل المقترحة. أخيراً كان هناك تطابق جيد بين النتائج العملية والنظرية للنموذج العددي وباختلاف يصل إلى (5%) كحد أقصى للفيض الحراري المسلط على السطوح المعرضة لأشعة الشمس.

1. Introduction

For most buildings, the earth acts as a heat sink continually conducting heat from the building foundation. The conduction heat transfer through the soil is governed by the soil thermal conductivity, which in turn depends primarily on three parameters: the soil type, the amount of moisture in the soil, and the soil temperature.

Bahnfleth (1989) ^[1] examined the influence of including solar and long-wave radiation and potential evaporation in the surface heat balance on soil temperatures and building heat loss via the ground. It was shown that the heat losses changed significantly when radiation or evaporation was included in the simulations. Shen (1986) ^[2] calculated the two-dimensional coupled heat and moisture transfer in soil near a basement wall. It was shown that the application of the uncoupled or the coupled equations for soil heat and moisture transfer leads to notably different basement wall heat losses. Rees et al. (2001) ^[3] analyzed the influence of the water height on the heat loss from earth-contact structures. Steady-state heat losses were calculated, which confined the considered coupling effects to the influence of soil moisture on the soil thermal conductivity. It was clearly demonstrated that the effect of soil moisture on building heat loss via the ground is not negligible, and deserves further attention. Deru (2001) ^[4] investigated the influence of precipitation on building heat loss via the ground. He concluded that soil moisture transfer has a notable influence on building heat loss via the ground.

Ground heat transfer modeling has usually assumed a given value of the soil thermal conductivity, constant soil properties, for calculation the surface energy balance, Deru and Kirkpatrick (2001) ^[5]. Building heat loss via the ground has consequently gained importance. This form of heat loss can no longer be considered an insignificant part of the overall building heat loss. One of the more important developments in this particular field is the ongoing improvement of the insulating quality of the building envelope. Deru et al. (2003) ^[6] developed a three-dimensional, finite-element; heat-transfer computer program to study ground- coupled heat transfer from buildings. It was used in conjunction with the SUNREL whole-building energy simulation program to analyze ground-coupled heat transfer from buildings. The results were compared with the simple ground-coupled heat transfer models used in whole-building energy simulation programs. The detailed model provides another method of testing and refining the simple models and analyzing complex problems.

Janssen et. al. (2004) ^[7] studied the influence of soil moisture transfer on building heat loss via the ground by comparing fully coupled simulations with linear thermal simulations.

The observed influences of coupling were (1) the larger amplitude of surface temperature, (2) the variation of thermal conductivity with moisture content, and (3) the advection of sensible heat by liquid transfer. In a parameter study, it was shown that these conclusions hold for a variety of climates, soils and foundation constructions. The transfer equations and boundary conditions are solved with a two-dimensional finite element spatial and a fully implicit time stepping scheme. Saati (2006) ^[8] used the finite difference scheme to study the effect of horizontal and vertical edge insulations on the heat transfer rate to the cold store through contact slab with the ground. The results showed almost a negligible change due to increasing the length of the horizontal edge insulation. In addition, increasing the length of the vertical insulation decreases the rate of heat transfer to the cold store. Therefore, the vertical insulation edge is economically recommended for use in cold stores in order to reduce the cooling capacity of the cooling machines.

Asslan (2007) ^[9] studied theoretically with a numerical method the effect of extended high thermal conductivity flat plate into ground for Iraqi buildings. He used an aluminum sheet with wall construction in the eastern and southern sides. With construction wall, it was used a layer of thermal insulation in different sites at the wall. The investigation showed that when using a plate only without insulation the cooling load is reduced by (13.2%) and (12.7%) for eastern and southern walls. Also, it showed that when using insulation the cooling load was reduced by (14.5%) and (15.8%) for southern and eastern walls respectively. This study was done on 21 July. Lu et al. (2007) ^[10] developed an improved model that describes the relationship between thermal conductivity and volumetric water at lower content in soils. With this new model, soil thermal conductivity can be estimated using soil bulk density, sand (or quartz) fraction and water content. They used for this study twelve type of soil. The results showed that the values of the model agree well with the measurements on all 12 media predicted. Another technique for utilizing from the regular temperature of ground was produced by Kerpel (2008) ^[11]. He presented a model for the calculation of the effectiveness of the earth-air heat exchanger (EAHE) with help of (TRNSYS) which is a dynamic simulation program for estimating the performance of any thermal system.

Tubes are installed under the ground through which air is drawn. At a certain depth, the ground temperature is lower than the outside air temperature in summer and higher in winter. When air is drawn through the pipe; it is cooled in summer and heated in winter. Thus the effectiveness for this model was assigned as:

$$\varepsilon = \frac{T_{air,out} - T_{air,in}}{T_{tubewall} - T_{air,in}} \dots\dots (1)$$

In the present work a new technique is suggested to be used for minimizing the cooling load by integrating the exposed eastern and southern walls, through a short circuit with the ground. Here, a metal sheet having high thermal conductivity is separated from these walls by an insulation material or air gap and extending it through the ground to a suggested depth of

(1) m. Further, a two dimensional numerical analysis was built to predict the transient temperature and heat flux variation through the space in Baghdad city.

2. Experimental Procedure

2-1 Experimental Room:

The experimental room was built with building common materials used in Iraq. It consists of walls and roof. Two of the walls are made of cork exposing to the north and west sides. The other two walls are built from multi layers with each layer having different thermal properties that composed the wall. The room's dimensions are 1m wide, 1m long and 1m high. The space walls are constructed of (20) mm gypsum on the inside, (240) mm common brick and (20) mm cement mortar on the outside for the eastern and southern directions. The roof is a flat having thickness of (10) mm made of concrete slab. The north side of room is supplied with a fan for ventilation. The floor of the room is compound of clay and layer of thin concrete, Ali (2009) ^[12].

Picture (1) shows the test room for the present experimental work objective. The earth under room was digged with one meter of depth and the plate is fixed on the wall. An air gap of (10) mm between the wall and the plate is allowed to prevent the conduction heat transfer between the plate and the wall.

2-2 Instrumentations

Measurements of temperature were done by (pt-100) type of thermocouples. All thermocouples are connected with the central reader consisting of selectors, contactors and digital reader; these thermocouples were calibrated against standard mercury thermometer with accuracies up to $(\pm 0.5)^\circ\text{C}$ for precise measurements. The digital reader also calibrated by connected it to a standard calibration reader. A portable digital thermometer has been used to measure the outdoor air. The chosen type of pt 100 sensor which is used for measuring the temperature has many favorite specifications. It has very short response time and has zero resistance which allow to high sensitivity in temperature measurement. Also, the range of its measuring temperature lies between $(-50 \text{ to } 200)^\circ\text{C}$. Therefore, it is most suitable for the present work from the other kinds of thermometers.

2-3 The Measurements

The experimental work consists of the measurement of room air temperature and inside and outside surfaces of the room with an earth-plate system and untreated room, before adding the metal sheet. Ambient temperature has also been monitored during the tests. Experiments were conducted continuously for the whole day in clear and sunny day during July 2008. The tests also conducted on different days chosen in July and August, the hottest months in Iraq, ^[12].



Picture (1): The Metal Sheet Fixed on the Wall.

3. Mathematical Model Formulation

Consider the three dimensional homogenous heat conduction equations in rectangular coordinate

$$\frac{\partial}{\partial x} \left(k_x \frac{\partial T}{\partial x} \right) + \frac{\partial}{\partial y} \left(k_y \frac{\partial T}{\partial y} \right) + \frac{\partial}{\partial z} \left(k_z \frac{\partial T}{\partial z} \right) + q = \rho C_p \frac{\partial T}{\partial t} \quad \dots (2)$$

The assumptions for modeling the heat transfer process in the wall are as following:

1. Conduction heat transfer is the major transfer mechanism.
2. The model is a two dimensional heat transfers, neglecting the heat transfer in the longitudinal direction. Assume for simplicity that all variables are constant in the z direction that is $(dT/dz) = 0$
3. The thermal properties in each layer of wall are assumed to be constant.
4. Generation of heat within building materials is in most cases not relevant; the generation of heat can then be put equal to zero ($q = 0$).
5. The problem is unsteady state (i.e. $\frac{\partial T}{\partial t} \neq 0$).
6. The solid material is isotropic; the thermal conductivity in each direction is constant.

Thus, when these assumptions are considered into account, eqn. (2) becomes:

$$\frac{\partial^2 T}{\partial x^2} + \frac{\partial^2 T}{\partial y^2} = \frac{1}{\alpha} \frac{\partial T}{\partial t} \quad \dots (3)$$

$$\alpha = \frac{k}{\rho \cdot C_p} \quad \dots (4)$$

Using an implicit finite differences, the terms in Equation (3) can be represented in terms of several grid points as follows:

The second-order derivatives in space and time are approximated using the central-differences

$$\frac{\partial^2 T}{\partial x^2} = \frac{T_{i+1,j}^{n+1} - 2T_{i,j}^n + T_{i-1,j}^{n+1}}{\Delta x^2} \quad \dots (5)$$

$$\frac{\partial^2 T}{\partial y^2} = \frac{T_{i,j+1}^{n+1} - 2T_{i,j}^n + T_{i,j-1}^{n+1}}{\Delta y^2} \quad \dots(6)$$

The first-order derivative in time is approximated using a forward-difference method:

$$\frac{\partial T}{\partial t} = \frac{T_{i,j}^{n+1} - T_{i,j}^n}{\Delta t} \quad \dots (7)$$

Substituting equations (5, 6, and 7) in (3):

$$\frac{T_{i+1,j}^{n+1} - 2T_{i,j}^n + T_{i-1,j}^{n+1}}{\Delta x^2} + \frac{T_{i,j+1}^{n+1} - 2T_{i,j}^n + T_{i,j-1}^{n+1}}{\Delta y^2} = \frac{1}{\alpha} \frac{T_{i,j}^{n+1} - T_{i,j}^n}{\Delta t} \quad \dots (8-a)$$

This leads to:

$$T_{i,j}^{n+1} = \frac{\alpha \cdot \Delta t}{\Delta x \cdot \Delta y} \left[\frac{\Delta y}{\Delta x} T_{i+1,j}^{n+1} + \frac{\Delta y}{\Delta x} T_{i-1,j}^{n+1} + \frac{\Delta x}{\Delta y} T_{i,j+1}^{n+1} + \frac{\Delta x}{\Delta y} T_{i,j-1}^{n+1} \right] + \left[1 - \frac{\alpha \cdot \Delta t}{\Delta x \cdot \Delta y} \left(2 \frac{\Delta y}{\Delta x} + 2 \frac{\Delta x}{\Delta y} \right) \right] T_{i,j}^n \quad \dots (8-b)$$

Equation (8-b) can solve all the internal nodes including the control volume of the system. On the external side of the room, the wall or the plate are exposed to the solar radiation and to convective heat transfer. Therefore, the external boundary condition at the outside wall of the space can be expressed mathematically as: $q_{conduction} = q_{convection} + q_{radiation}$

$$-\left(k \frac{\partial T}{\partial x} \right) = h_o (T_w - T_\infty) + \alpha q_r \quad \dots (9)$$

On the internal side, the room wall exposed to the inside environmental.

$$q_{conduction} = q_{convection}$$

$$-\left(k \frac{\partial T}{\partial x}\right) = h_i (T_w - T_\infty) \quad \dots (10)$$

The heat flow by convection can be calculated as follows:

$$Q = A h (T_o - T_{os}) \quad \dots (11)$$

The absorbed heat in a surface j due to solar radiation is estimated as follows

$$I_j = \alpha \cdot A \cdot I_t \quad \dots (12)$$

It is possible to calculate the various heat exchanges taking place in a building. The rate of heat conduction (Q_{cond}) through any element such as roof, wall or soil under any condition can be written as:

$$Q_{cond} = A U \Delta T \quad \dots (13)$$

Where (U) is given by:

$$U = \frac{1}{\sum R_t} \quad \dots (14)$$

$$R_t = \frac{1}{h_i} + \left(\sum_{j=1}^m \frac{L_j}{k_j} \right) + \frac{1}{h_o} \quad \dots (15)$$

(h_i) and (h_o) are the inside and outside heat transfer coefficients respectively. In this study, it was assumed that $h_i=8.29$ and $h_o= 22.71$ ($W/m^2.C$), ASHRAE (1997) ^[13]. (L_j) is the thickness of the (j th) layer and (k_j) is the thermal conductivity of its material. If the surface is exposed to solar radiation then,

$$\Delta T = T_e - T_i \quad \dots (16)$$

Where (T_i) is the indoor temperature and (T_e) is the sol-air temperature, calculated by using the expression, ^[13]:

$$T_e = T_o + \frac{\alpha I_t}{h_o} - \frac{\epsilon \Delta R}{h_o} \quad \dots (17)$$

Where (α) is absorptance of the surface for solar radiation. For this study, it was chosen to be $\alpha=0.6$, BIS (1987) ^[14]. (ΔR) is the difference between the long wavelength radiation incident on the surface from the sky and the surroundings, and the radiation emitted by a black body at ambient temperature. For vertical surface, $\Delta R=0$; equation (17) becomes:

$$T_e = T_o + \frac{\alpha \cdot I_t}{h_o} \quad \dots (18)$$

4. Soil Thermal Conductivity:

In this paper, the most widely accepted physical model for soil thermal conductivity was derived by De Vries ^[15] is used. For moist soils, he assumed the liquid phase as a continuous medium in which solid grains and small air pockets are uniformly distributed. The overall thermal conductivity of soil is calculated as the weighted average of the conductivities of the various soil components according to the formula:

$$k = \frac{\sum_{i=0}^n k_i x_i \lambda_i}{\sum_{i=0}^n x_i \lambda_i} \dots (19)$$

Where (x_i) is the volume fraction of each constituent, and (n) is the number of soil constituent.

The weighting factor (λ_i) depends on the shape and the orientation of the granules of the soil constituents, and on the ratio of the conductivities of the constituents. It can be calculated as:

$$\lambda_i = \frac{1}{3} \sum_{j=1}^3 \left[1 + \left(\frac{k_i}{k_o} - 1 \right) g_j \right]^{-1} \dots (20)$$

The subscript zero refers to the continuous fluid surrounding the solid particles (air for dry soil and water for moist soil), $\lambda_o = 1$.

Where (g_j) represents the shape factors for the i -th constituents granules considered as ellipsoids,

$$g_1 + g_2 + g_3 = 1 \text{ (for each component), } [15]. \dots (21)$$

Assuming (g_1) and (g_2) are equal; only one shape factor must be estimated for each constituent.

The thermal conductivity of water is (0.596) W/m K at (20) °C. The thermal conductivity of the air is (0.025) W/m K at the same condition.

The shape factor, (g_1) for the soil solids was taken to be (0.144), Tyson et al. (2001) [16]. For water contents; the value of (g_1) is given by:

$$g_1 = 0.333 - \frac{x_a}{1 - x_s} (0.333 - 0.035) \dots (22)$$

These equations are solved numerically in a fully implicit scheme, using initial temperature distribution of (25) °C, the resulting set of equations were solved by MATLAB, Ali (2009) [12]. Figure (1) shows the dimensions and coordinates of the system used for the simulation strategy in the present work.

5. Results and Discussion

Figure (2) shows the effect of using metal sheet with exterior building wall on the indoor temperature. It can be seen that, there is a difference between temperature swings of the indoor temperature to time lag. Without using a metal sheet, the maximum indoor temperature reaches up to $(34.5) ^\circ\text{C}$. While this value becomes lower by applying a metal sheet and can approach $(31.7) ^\circ\text{C}$ with air gap including a reduction percentage of (8.1%) and to $(29.9) ^\circ\text{C}$ when using glass wool corresponds to a reduced percentage of (13.3%). This will improve designs for energy efficient buildings with comfortable indoor temperature and will reduce the duration of uncomfortable periods.

Figures (3 and 4) show the effect of using a metal sheet with an air gap and glass wool through southern wall on the heat flux transmitted to the room. The same phenomena of damping and time shifting can be observed in the heat fluxes. The heat flux at the outdoor surface without plate and insulation changes dramatically during the day and reveals a peak at (1:00 p.m). It is obvious from the two figures that there is a significant difference in the maximum value of heat flux due to using a metal sheet. The use of air space is to prevent or reduce a noise to the space and it is a good insulation.

According to thermal conductivity of the insulation material, there is a variation in heat flux. The thermal conductivity of glass wool is lower than that of air i.e., glass wool has thermal resistance higher than that of air space. Therefore, the heat flux flowing into the inner surface of a south-facing wall insulated with glass wool is lower than that of a wall insulated with air space. The maximum heat flux through the wall without a plate is $(61.1) \text{ W/m}^2$. This amount decreases to $(46.7) \text{ W/m}^2$ in the case of insulated wall with air gap with a reduce percentage reaches to (23.5%) and to $(40.5) \text{ W/m}^2$ with a reduced percentage reaches to (33.7%) in the case of insulated wall with glass wool.

Figures (5 and 6) illustrate the effect of using a metal sheet with an air gap and glass wool through eastern wall on the heat flux. The maximum heat flux without metal sheet reaches to $(53.6) \text{ W/m}^2$. This maximum heat flux will reduce to $(42.7) \text{ W/m}^2$ when using air gap with the metal sheet and this value will become $(38.4) \text{ W/m}^2$ when using glass wool instead of air gap. The reduction percentage for both two cases is (23.5%) and (28.3%) respectively. The decreasing in heat flux may be useful for saving the energy and dropping the cooling load in the Iraqi building.

Figure (7) shows the temperature distribution in the southern wall without using the metal sheet represented with a three dimensions. The behavior revealed that the temperature profile drops slowly and this drop is proportional to the position through the depth of wall. The slope of dropping is not constant; it varies from one material to another according to the thermal properties of each material. The coordinate (depth) represents the thickness of wall starting from the inside wall at depth coordinate of (21) cm and extended to (50) cm where the total thickness of the wall will equal to (29) cm including the air gap or insulation thickness.

Figure (8) shows the comparison between theoretical and experimental outside surface temperature at the east side without using metal sheet. There is a good agreement between the predicted and measured behaviors. The maximum temperature is $(51)^{\circ}\text{C}$ while the minimum is $(33.5)^{\circ}\text{C}$ appears at (5 a.m). Figure (9) compares the inside eastern surface temperature for both experimental and theoretical behavior without using metal sheet. It is obvious that the maximum theoretical temperature is $(34)^{\circ}\text{C}$ at (1p.m) while the maximum experimental temperature reaches to $(33)^{\circ}\text{C}$. The difference between maximum theoretical and experimental temperatures reaches to $(1)^{\circ}\text{C}$ with accuracy limit of (2.94%).

Figure (10) shows the temperature distribution in the southern wall when using the metal sheet represented as a three dimensional graph. It is clear, that the highest temperature occurs at aluminum surface .At the interface of metal sheet, the temperature will drop with a high slope. At the air gap interface with wall, the temperature is $(51.5)^{\circ}\text{C}$. The maximum values of surface temperature is a function of position through the wall. It decreases as thickness of the wall increase, towards the outside, and the minimum values increase as wall thickness increase. The metal sheet will reduce the heat flux on the building allowing reduction in the cooling load. Figure (11) explains with a 3-D representation the shape of the temperature distribution in the eastern wall when using a metal sheet with air gap insulation. It can be seen that the curve of temperature at any point takes the sine wave with a different amplitudes and the amplitude decrease as the depth of wall is increased, towards the outside surface. The temperature of aluminum surface reaches to $(57)^{\circ}\text{C}$.

Figure (12) illustrates the behavior of the predicted temperature in the outside southern structure wall with and without using metal sheet and for two types of insulation, air gap and glass wool. There is an apparent difference in the maximum temperature recorded. The maximum temperature without metal sheet reaches to $(57.5)^{\circ}\text{C}$, this value was reduced to $(51.5)^{\circ}\text{C}$ when using metal sheet with air gap with a reduced percentage of (10.4%) and to $(45.5)^{\circ}\text{C}$ with a reduced percentage of (20.8%) when using metal sheet with glass wool. This shows the effect of the insulation efficiency on the temperature distribution through the building wall and hence the heat rate absorbed by the building and the efficiency of the metal sheet on the overall cooling load.

6. Conclusions

Regarding to the influence of a geothermal system, the theoretical and experimental work has indicated the following conclusions:

1. The geothermal system has a significant effect in reducing indoor temperature in the space compared without using it. When the metal sheet was used in combination with the air gap and glass wool, the heat flux for the eastern wall was reduced by (23.5%) and (28.3%) respectively. The corresponding values for the southern wall were (23.5%) and (40.5%) respectively.
2. Since south and east faces receive amount of incident solar radiation more than north and west, it is more effective to use the plate in the south and east sides.
3. In order to decrease the cooling load in the building in hot zones, an insulation has high thermal conductivity should be avoided since it allows a highest heat gain.
4. The theoretical prediction obtained from the present model showed a good agreement with the experimental data and a two dimensional heat transfer model is enough to satisfy the simulation object.
- 5.

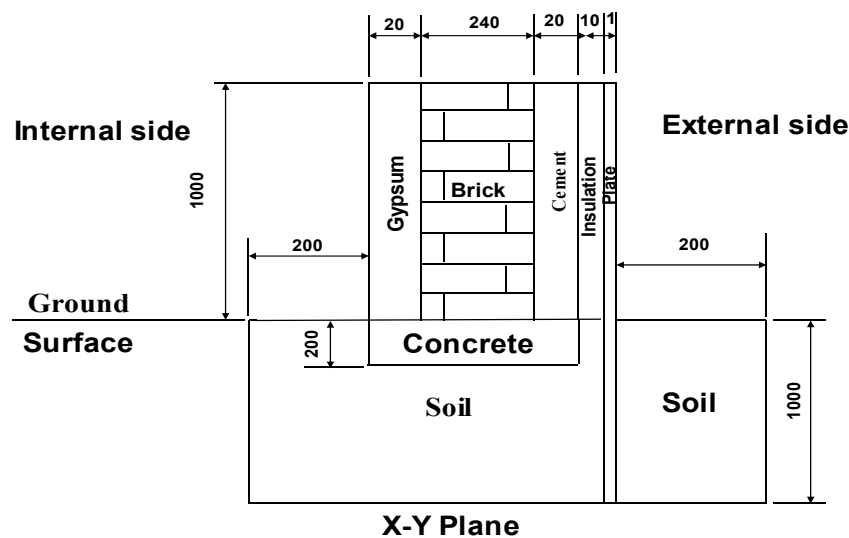


Figure (1): The physical Model with Dimensions in (mm).

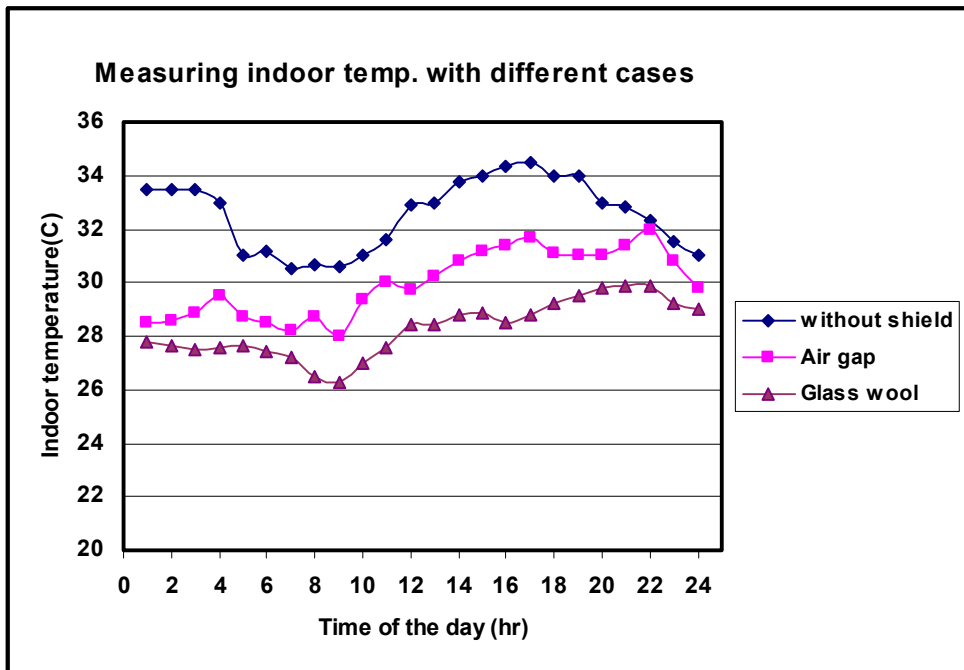


Figure (2): A Comparison of the Indoor Temperature Variation with Time for Different Conditions.

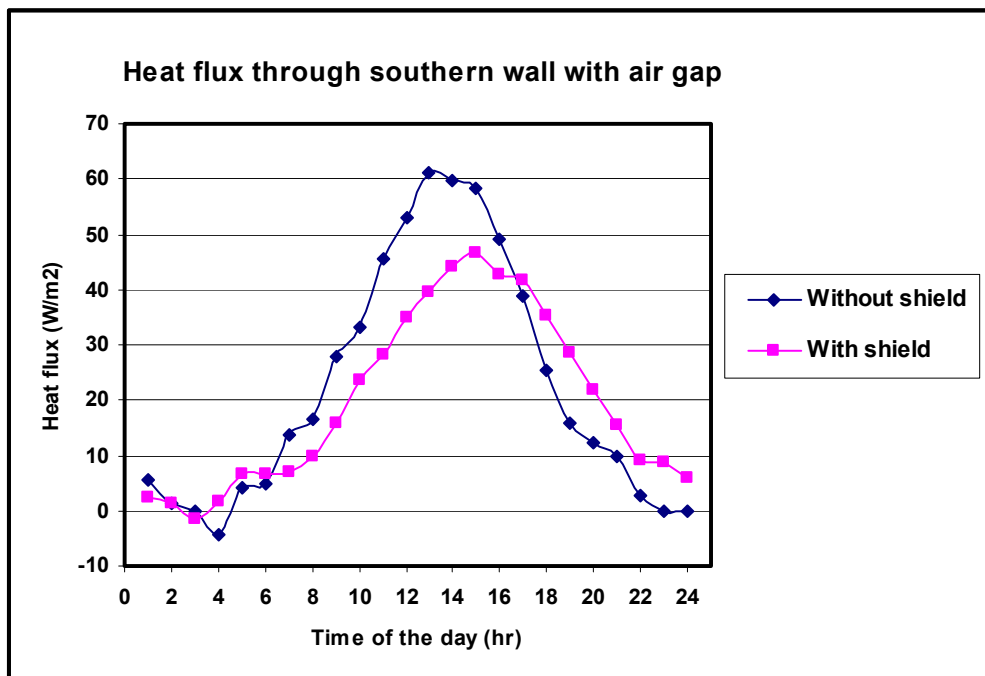


Figure (3): The Effect of Using a Metal Sheet with Air Gap on the Heat Flux Through the Southern Wall 20- July.

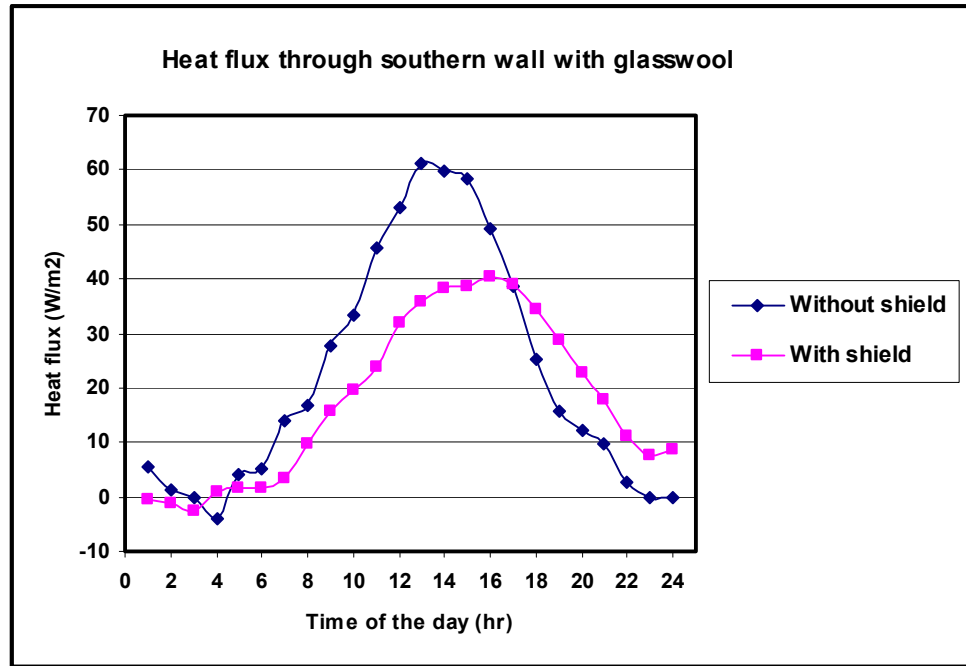


Figure (4): The Effect of Using a Metal Sheet with Glass Wool on the Heat Flux Through Southern wall 22- July.

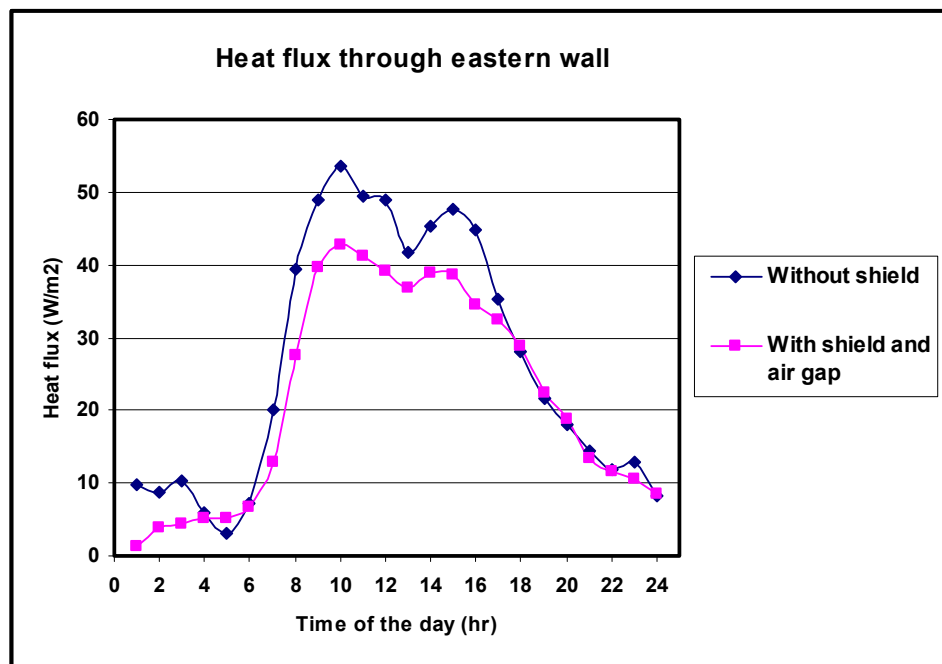


Figure (5): The Effect of Using a Metal Sheet with Air Gap on the Heat Flux Through Eastern Wall 20- July.

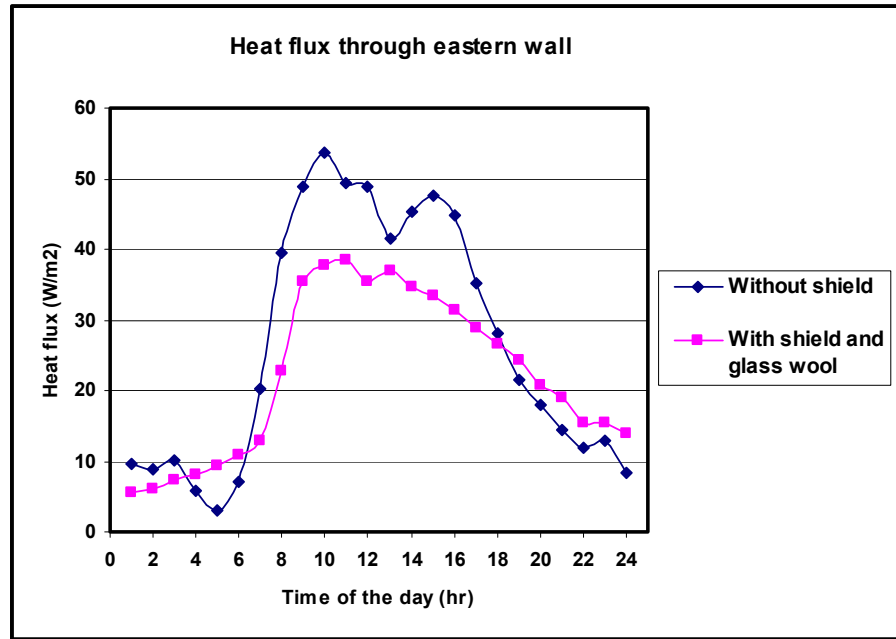


Figure (6): The Effect of Using a Metal Sheet with Glass Wool on the Heat Flux Through Eastern Wall on 22- July.

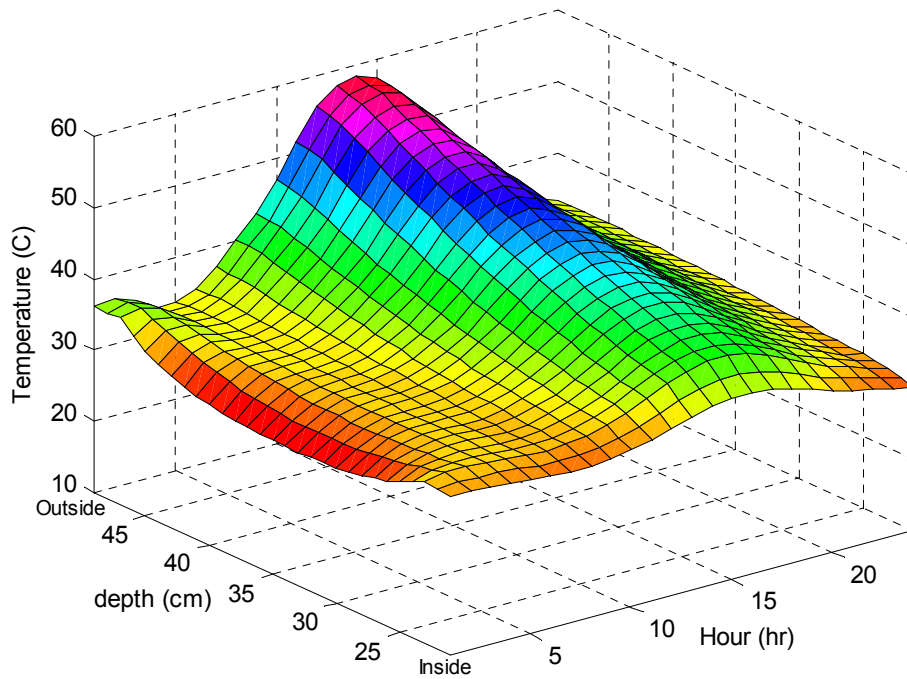


Figure (7): The Temperature Distribution in the Southern Wall without

Using Metal Sheet.

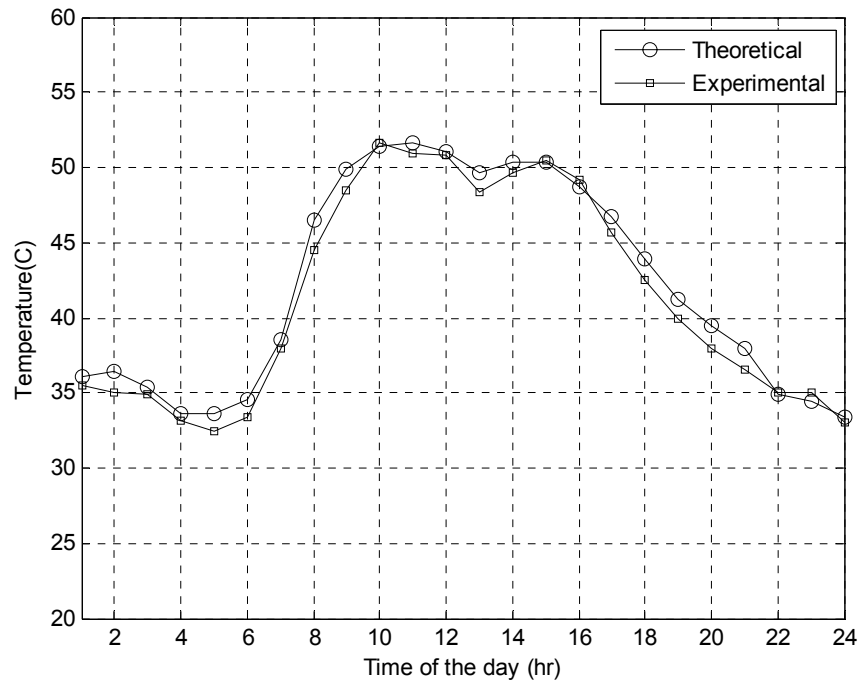


Figure (8): A Comparison Between Theoretical and Experimental Outside Surface Temperature at the East Side without Using Metal Sheet.

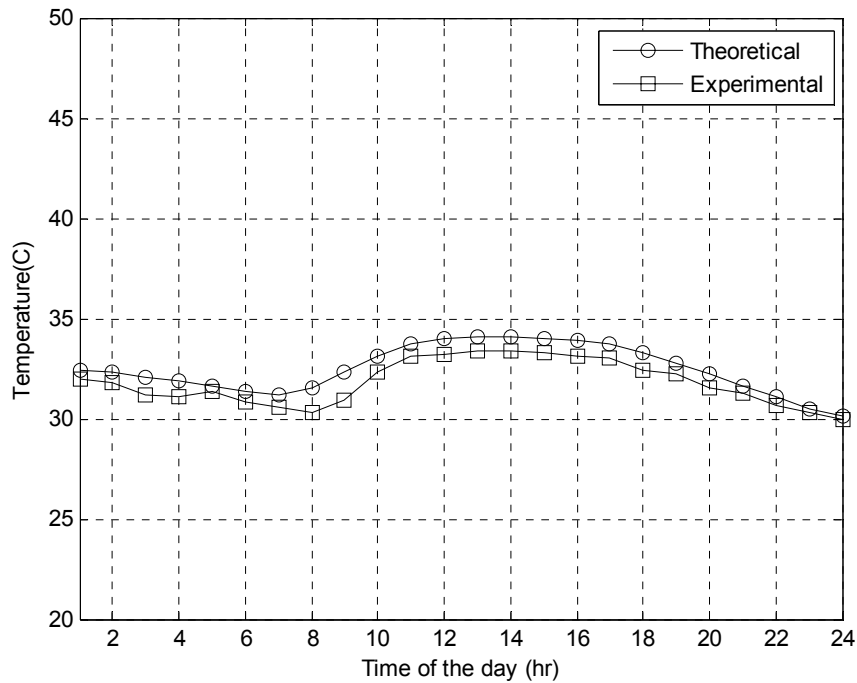


Figure (9): A Comparison Between Theoretical and Experimental Inside Wall Surface Temperature at the East Side without Using Metal Sheet.

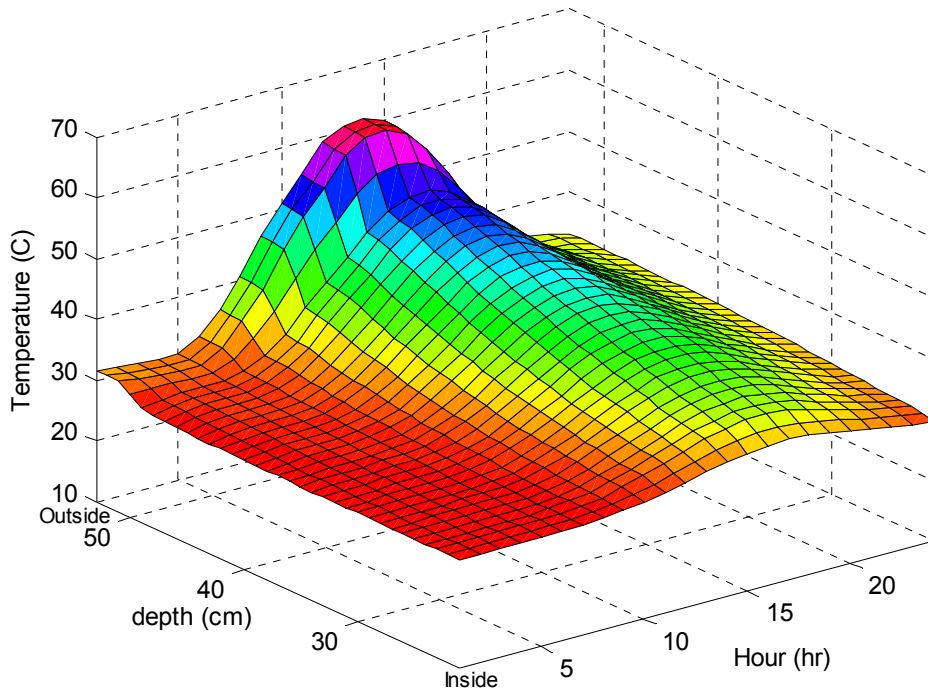


Figure (10): The Temperature Distribution in the Southern Wall Using Metal Sheet with Air Gap Insulation.

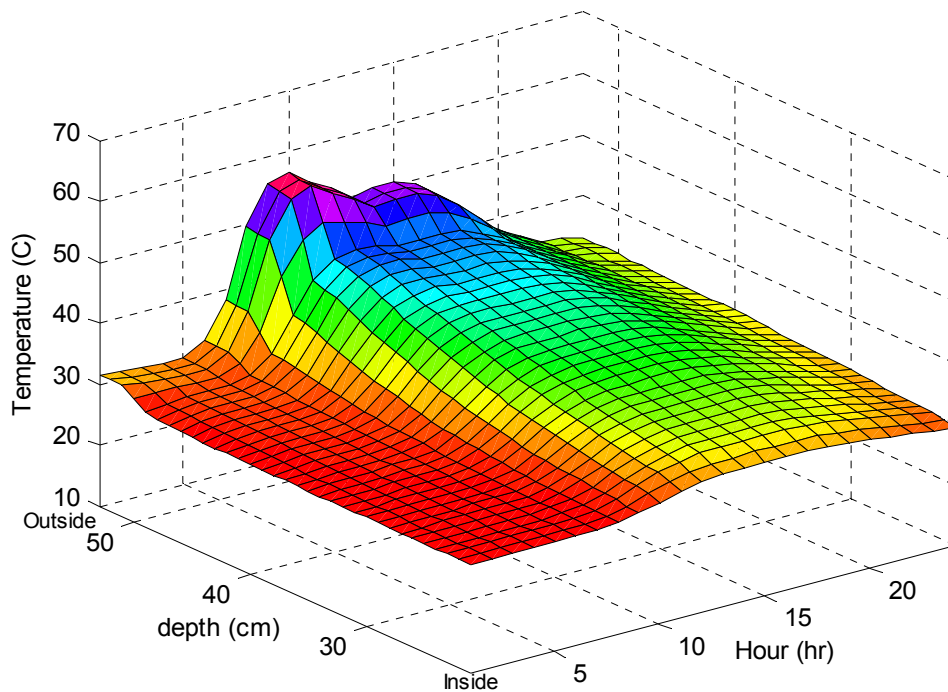


Figure (11): The Temperature Distribution in the Eastern Wall Using Metal with Air Gap Insulation.

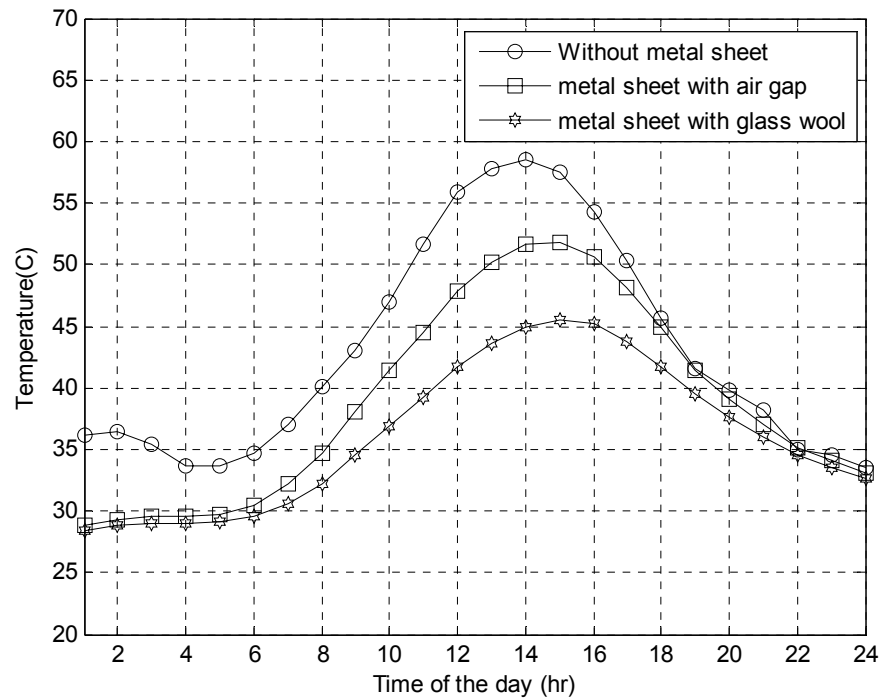


Figure (12): The Temperature Predicted in the Outside Southern Wall Using Metal Sheet with Insulation

Nomenclature

A :	surface area,	m^2
g_j :	shape factor,	-
h_i :	inside heat transfer coefficients respectively,	$W/m^2 \cdot ^\circ C$
h_o :	outside heat transfer coefficients respectively,	$W/m^2 \cdot ^\circ C$
i :	numerical index in X-direction,	-
I_t :	total solar flux on an incident surface,	W/m^2
j :	numerical index in Y-direction,	-
K :	thermal conductivity,	$W/m.K$
n :	number of soil constituents,	-
Q :	heat flow,	W
R :	thermal resistance,	$m \cdot ^\circ C / W$
t :	time,	s
T :	temperature ,	$^\circ C$
T_e :	sol-air temperature ,	$^\circ C$
T_i :	initial temperature,	$^\circ C$
U :	overall thermal transmittance,	$W/m^2 \cdot ^\circ C$
x_i :	volume fraction of each constituent for soil ,	-
x_s :	volume fraction of solid ,	-
x_a :	volume fraction of air,	-

Greek letters

α :	absorptive,	-
λ_i :	weighting factor	-

7. Reference

1. Bahnfleth, W. P.: *"Three-Dimensional Modeling of Heat Transfer from Slab Floors"*, National Technical Information Service, Springfield, VA, ADA210826, (1989).
2. Shen, L. *"An Investigation of Transient, Two-Dimensional Coupled Heat and Moisture Flow in Soils"*, Doctoral Dissertation, University of Minnesota, United States, (1986).
3. Rees, S., Zhou, Z. and Thomas, H.R.: *"The Influence of Soil Moisture Content Variations on Heat Losses from Earth-Contact Structures: An Initial Assessment"*, Building and Environment J. Vol.36, pp. (157–165), (2001).
4. Deru, M.: *"A Model for Ground-Coupled Heat and Moisture Transfer from Buildings"*, Doctoral Dissertation, Colorado State University, United States, (2001).
5. Deru, M. P. and Kirkpatrick, A.T., *"Ground-Coupled Heat and Moisture Transfer from Buildings"*, American Solar Energy Society (ASES), (2001).
6. Deru, M., Judkoff, R. and Neymark, J.: *"Whole-Building Energy Simulation with a Three-Dimensional Ground-Coupled Heat Transfer Model"*, Chicago, (2003).
7. Janssen, H. J., Carmeliet, D. and Hens, H., *"The Influence of Soil Moisture Transfer on Building Heat Loss via the Ground"*, Building and Environment, J. Vol. 39, pp. (825–836), (2004).
8. Saati, A. A., *"A Numerical Investigation of Ground Heat Transfer Effects on Buildings Including Edge or Composite Slab Insulation"* Umm Al-Qura Univ. J. Sci. Med. Eng., Vol. 18, No.1, pp. (73 -88), (2006).
9. Asslan, M.A., *"Numerical Study for a New Geothermal System to Reduce Cooling Load in Iraqi Buildings"*, MSc. Thesis, university of technology, Baghdad, (2007).
10. Lu, S., Ren, T., Gong, Y. and Horton, R., *"An Improved Model for Predicting Soil Thermal Conductivity from Water Content at Room Temperature"*, Soil Sic. Soc. Am. J., Vol. 71, pp. (8-14), (2007).

11. Kerpel, D. D., *"Evaluation of Models for the Calculation of Earth-Air Heat Exchange"*, electromechanical engineering dept., Ghent University, Belgium, (2008).
12. Ali, W. A., *"The Effect of Thermal Properties of Building Materials on the Application of the Geothermal Heat Storage Phenomenon in Cooling Load of a Space"*; M.Sc. Thesis, Al-Mustansiriya University, Baghdad, (2009).
13. ASHRAE, Handbook, *"The American Society of Heating, Refrigerating and Air-Conditioning Engineers"*, Fundamentals, Ch.29, (1997).
14. Bureau of Indian of Standards, *"Handbook on Functional Requirements of Buildings"*, New Delhi, (1987).
15. De Vries, D.A., *"Thermal Properties of Soils"*, Physics of the plant environment, North-Holland, Amsterdam, (1966).
16. Tyson, E., Horton, O. R. and Tusheng, R., *"A New Perspective on Soil Thermal Properties"*, Soil Sci. Soc. Am. J. Vol. 65, pp. (1641–1647), (2001).